Chapter 8
Engine Limit Management with Sliding Modes

Abstract This chapter develops a method to maintain critical engine variables within allowable limits, without the disadvantages associated with the standard min–max approach. Guidelines for the association of sliding mode regulators to logic max or min selectors are given, along with an $\mathcal{H}_2/\mathcal{H}_\infty$ sliding coefficient synthesis method. Simulations using the CMAPSS nonlinear engine model are included.

Sliding modes constitute a powerful tool to achieve the simultaneous objectives of robust output regulation and limit protection. Research conducted by the author in collaboration with NASA [73] indicate that many shortcomings of the standard min–max approach can be removed by replacing linear regulators with SMC. A single-input version of the *max-min/SMC* approach was available at the time this book was printed, and is presented in this chapter. Thus, the developments of this chapter assume that only one input is available to manage both regulation and limit protection objectives.

The central idea of the max–min/SMC approach is to *define sliding functions as the difference between a limited variable and its permissible limit*. One of such functions is defined for each limited output, in addition to a sliding function defined for the main regulated output (fan speed in the GTE problem). Recalling from Chap. 6 that since convergence of the s variable to zero is one-sided, if follows that outputs will not cross their limits when their corresponding SMC regulator is active.

Remarkably, the technique also assures that outputs will not cross their limits even when some other regulator is active. This represents a significant improvement over the min–max arrangement with linear regulators of Chap. 7, where transient limit protection cannot be guaranteed.

Establishing stability is of the utmost importance for the development of new control laws. In the max–min/SMC approach, asymptotic stability is guaranteed, ensuring that suitably-defined error states converge to zero. The approach constitutes a *hybrid dynamical system*, in that discrete variables exist that interact with the continuous system state. The relevant discrete variable in the max–min/SMC

H. Richter, *Advanced Control of Turbofan Engines*, DOI 10.1007/978-1-4614-1171-0_8,

approach is q, the index of the currently active SMC regulator. This variable takes on integer values, reflecting the number of regulators being implemented. A notion of stability must also be considered for q. The max-min/SMC approach has the property that q undergoes a finite number of transitions before it settles at a steady value.

The limit-preserving and stability properties of the max–min/SMC approach are ensured by following simple guidelines for associating regulators with the max or min selectors, and then tuning each SMC regulator independently. That is, a *separation property* applies, akin to the well-known property of linear observers used in combination with linear state feedback control [65]. Note that the sliding coefficients corresponding to the SMC limit regulators are no longer design freedoms: they are defined by the C matrix of each limited output. Because of this, the technique is applicable to *minimum-phase outputs* only, since the eigenvalues of the matrix defining sliding mode dynamics coincide with the zeroes of the transfer function from input to limited output. The reader may wish to re-visit Chap. 3, where the effects of right-half plane zeroes are discussed. Thus, limit regulator design entails the selection of switching gains η and boundary-layer parameters ϕ. The sliding coefficients corresponding to the main SMC regulator are design freedoms, as elaborated below. Basic design is conducted by choosing these coefficients on the basis of the main output regulation task alone. An advanced design technique is also possible, where interaction between main and limit regulators is addressed in a mixed $\mathcal{H}_2/\mathcal{H}_\infty$ synthesis framework similar to that of Chap. 4.

The detailed stability argument for max–min/SMC is involved and out of the scope of this book. Interested readers are referred to Richter [59] for a complete mathematical proof. Here, the control law is developed and the salient stability and limit-preservation properties are described.

8.1 System Description, Assumptions and Control Objectives

The architecture of max–min/SMC is the same as the max–min arrangement of Chap. 7, with the linear regulators replaced by sliding mode regulators, as illustrated in Fig. 8.1.

Due to the requirement that the main output be precisely regulated, integration is used at plant input. The regulators, thus, provide control input rates. Letting $L = \{1, 2, ...l\}$ and $H = \{l + 1, l + 2, ...h\}$, the max–min selection law is expressed as

$$u_r = \max_{k \in H} \left\{ \min_{j \in L} \left\{ u_{\mathrm{rj}} \right\}, \quad u_{\mathrm{rk}} \right\}, \tag{8.1}$$

where u_{rj} are the min-linked regulator outputs and u_{rk} are the max-linked regulator outputs. Some studies characterizing the behavior of related schemes have appeared

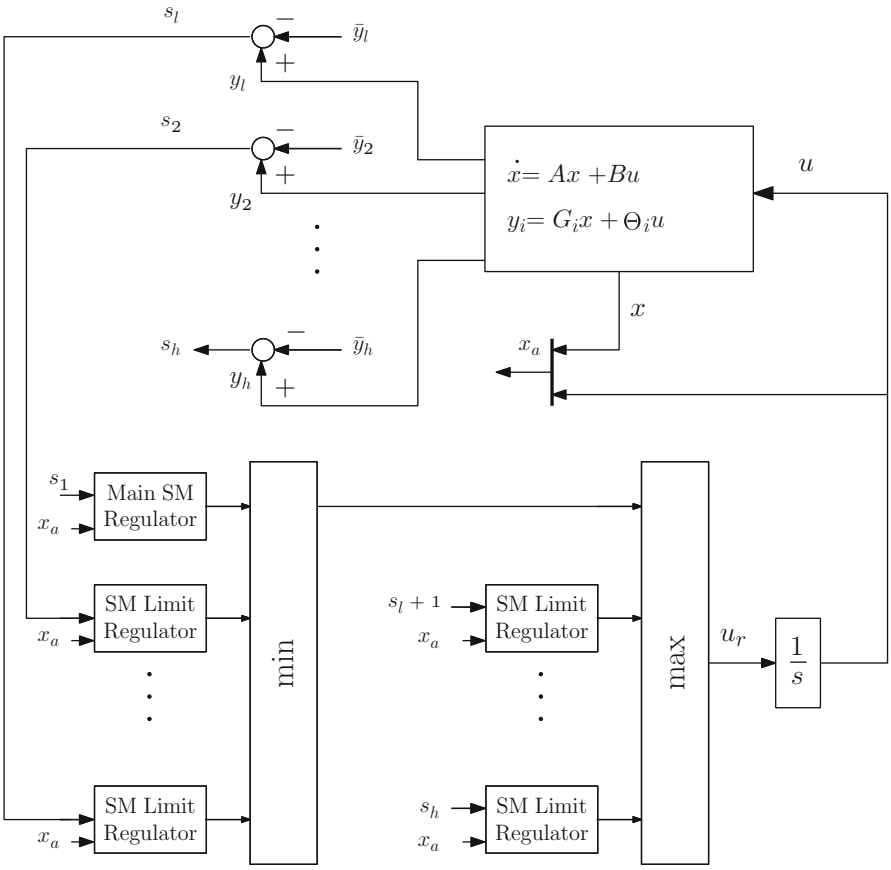

Fig. 8.1 Max-Min/SMC arrangement

in the research literature [66–68]. Recently, the (nonasymptotic) stability of this particular scheme under linear regulators has been analyzed by Johansson [33] using piecewise-quadratic Lyapunov functions. Even for linear regulators, a complete characterization of closed-loop behavior that includes essential issues such as determining which regulator will be active at steady-state or how to design the regulators to address performance requirements does not exist in the open literature. Limit protection is an indispensable consideration in the GTE problem; however, few works addressing the max–min arrangement have appeared [64, 69]. Of particular importance is the observation that limit regulators may become active even when the auxiliary outputs are far from their limits, causing a degradation in the response of the main output due to an overriding control objective [69]. Also, as established in Chap. 7, the max–min architecture with linear regulators does not ensure transient limit protection, a less-than-desirable feature.

We consider linearized models for the engine, with a single control input u (typically fuel flow). Considering that the controller includes integral action, the state-space description of the design plant is:

$$\dot{x} = Ax + Bu + \Gamma w \tag{8.2}$$

$$\dot{u} = u_r, \tag{8.3}$$

where x is n-by-1 and u and u_r are scalars. The above model captures the effect of uncertainties and exogenous inputs through vector w and its input matrix Γ, of compatible dimensions. Assume that a set of outputs is defined as

$$y_i = G_i x + \Theta_i u \tag{8.4}$$

for $i = 1, 2, ...h$, with G_i a 1-by-n vector and Θ_i a scalar.

We make three key assumptions: A is nonsingular, $\Theta_i \neq 0$ and matrices $A_{\text{eq}.i}$ defined in (8.5) have eigenvalues with negative real parts for $i = 1, 2, ...h$.

$$A_{\text{eq},i} = A - \frac{BG_i}{\Theta_i}. \tag{8.5}$$

The assumption on $A_{\text{eq},i}$ is equivalent to the requirement that the outputs defined by (8.4) are minimum-phase relative to the state-space system of (8.2). Note that when A contains a zero eigenvalue, the corresponding integrator can be factored out from the transfer function between u and y_i, resulting in a nonsingular A. The input integrator is not implemented explicitly as part of the control law. When $\Theta_i = 0$ for some i, further modifications are required [59].

8.1.1 Control Objectives

Without loss of generality, let y_1 be the output whose setpoint is to be transferred with zero steady-state error. This must be achieved under constraints of the form $y_k \leq \bar{y}_k$ and $y_l \geq \bar{y}_l$, where k are the indices of the upper-limited outputs and l are the indices of the lower-limited outputs. In addition, usual transient response specifications apply for the design of the main output regulator.

8.1.2 Sliding Mode Control Laws

Define sliding variables as

$$s_i = y_i - \bar{y}_i \tag{8.6}$$

for $i \in L \cup H$, where $\bar{y}_i = G_i \bar{x}_i + \Theta_i \bar{u}_i$. The reference variables $\bar{x}_i$ and $\bar{u}_i$ are selected to be equilibrium pairs, that is, so that $A\bar{x}_i + B\bar{u}_i = 0$. The standard SMC control law is obtained by requiring that $s_i = 0$ in finite time (reaching

phase). Beyond the reaching phase, $s_i = 0$ must become invariant (sliding phase). The system then evolves with reduced-order dynamics matching the zero dynamics associated with output s_i. Thus, a minimum-phase assumption is required. For a single SMC regulator (fixed i), the control law given below in (8.7), where η_i is a positive constant, forces the function $\frac{1}{2}s_i^2$ to have derivative $s_i\dot{s}_i = -\eta_i \text{ sign } (s_i)$. implying that the set $s_i = 0$ is reached in finite-time, with subsequent invariance.

$$u_{\text{ri}} = -\frac{1}{\Theta_i}\left(G_i(Ax + Bu) + \eta_i \text{ sign } (s_i)\right) \tag{8.7}$$

In view of the definition of s_i, a limit regulator, if operated alone, causes its corresponding limited output to attain the limit value in finite time without overshoot. Under the max–min selection logic, the closed-loop system is given by (8.2), (8.3), (8.4), (8.6), (8.7), and (8.1). The controller implements (8.6), (8.7), (8.1), and (8.3).

8.2 Behavior Under a Fixed Regulator

Let i and j be two fixed regulator indices and define the augmented state as $x_a \triangleq [x^T|u]^T$, let $\bar{x}_{\text{ai}} = [\bar{x}_i^T|\bar{u}_i]^T$ and define the augmented state relative to i as $\tilde{x}_a \triangleq x_a - x_{\text{ai}}$. Using this definition, it is straightforward to derive the following identities pertaining to system behavior under the control law of (8.7):

$$\dot{\tilde{x}}_a = A_i\tilde{x}_a - \frac{1}{\Theta_i}B_i\eta_i \text{ sign } (s_i) \tag{8.8}$$

$$s_j = J_j\tilde{x}_a + \Delta_{j,i} \tag{8.9}$$

$$\dot{s}_{j|i} = \Theta_j\left(\Gamma_{j,i}\tilde{x}_a - \frac{\eta_i}{\Theta_i}\text{ sign } (s_i)\right). \tag{8.10}$$

where:

$$A_i = \begin{bmatrix} A & B \\ -\frac{G_i}{\Theta_i}A & -\frac{G_i}{\Theta_i}B \end{bmatrix}, \quad B_i^T = [0_{1\times n}|1] \tag{8.11}$$

$$J_j = [G_j|\Theta_j], \quad \Delta_{j,i} = J_j(\bar{x}_{\text{ai}} - \bar{x}_{\text{aj}}) \tag{8.12}$$

$$\Gamma_{j,i} = \left[\frac{G_j}{\Theta_j} - \frac{G_i}{\Theta_i}\right]\left[A\middle|B\right] \tag{8.13}$$

The notation $\dot{s}_{j|i}$ is interpreted as "the derivative of s_j when i is the active regulator". When $i = j$, we simply write $\dot{s}_i$. Note that $\Delta_{i,i} = 0$ and $\Gamma_{i,i} = 0$ for $i \in L \cup H$. It follows from standard sliding mode theory that for each i, the

spectrum of A_i is formed by the eigenvalues of $A_{\text{eq},i}$ from (8.5) and zero. The closed-loop system resulting from applying the input of (8.7) to system (8.2), (8.3) is more conveniently described in terms of the derivatives of the s variables, as before, and the *rate* of x. In fact, define $X_r \triangleq \dot{x}$. The closed-loop system dynamics are expressed as

$$\dot{X}_r = A_{\text{eq},i} X_r - B \frac{\eta_i}{\Theta_i} \text{ sign } (s_i) \tag{8.14}$$

$$\dot{s}_{j|i} = \Theta_j \left[\left(\frac{G_j}{\Theta_j} - \frac{G_i}{\Theta_i} \right) X_r - \frac{\eta_i}{\Theta_i} \text{ sign } (s_i) \right]. \tag{8.15}$$

The rate system is a convenient description, since $A_{\text{eq},i}$ characterizes the dynamics of the sliding mode, facilitating the description of asymptotic properties.

8.2.1 Determination of the Steady Regulator Index

Define a switching function $q(x, u)$ with values in $L \cup H$. The minimum (min), maximum (max) switching functions are expressed by (8.16) and (8.17), respectively.

$$q_{\min} = \underset{i \in L}{\arg\min} \{u_{\text{ri}}\} \tag{8.16}$$

$$q_{\max} = \underset{j \in H}{\arg\max} \{u_{\text{rj}}\}. \tag{8.17}$$

When the above equations yield nonunique values, an assignment is made according to a predefined arbitrary rule. For the remainder of this chapter, $q_{\min} = \min(i, j)$ and $q_{\max} = \min(i, j)$ are assumed whenever $u_{\text{ri}} = u_{\text{rj}}$. When a max–min arrangement is used, it is assumed that the min preselection is applied to the first port of the max selector, so that the min input is used in case of equality with the max preselection. These assumptions will be referred to as *default index assumptions*.

As done for the max–min arrangement for linear regulators of Chap. 7, a procedure to determine the steady regulator index is developed next.

Under the min switching law, system (8.2), (8.3) has a unique equilibrium point at $(\bar{x}_{i^*}, \bar{u}_{i^*})$, where $i^* \in L$ is the index such that $\frac{\text{sign } (\Delta_{j,i^*})}{\Theta_j} \leq 0 \; \forall j \in L$.

Given system parameters, it is straightforward to compute the terminal regulator index. All $\Delta_{j,i}$ combinations are computed. For the min law, an index i^* is sought that satisfies $0 \leq -\frac{\eta_j}{\Theta_j} \text{ sign } (\Delta_{j,i^*})$ for all $j \in L, \; j \neq i^*$.

Under the max switching law, system (8.2), (8.3) has a unique equilibrium point at $(\bar{x}_{i^*}, \bar{u}_{i^*})$, where $i^* \in H$ is the index such that $\text{sign}\,(\Delta_{j,i^*}) \geq 0\ \forall\, j \in H$. This index is termed *terminal regulator index*.

The determination of the terminal index for the max and max–min switching laws is presented next.

Under the max–min switching law of (8.1), system (8.2), (8.3) has a unique equilibrium point at $(\bar{x}_{i^*}, \bar{u}_{i^*})$, where $i^* \in L \cup H$ is the index satisfying condition (8.18):

$$0 \geq -\frac{\text{sign}\,(\Delta_{k,i^*})}{\Theta_k} \quad \forall k \in H \tag{8.18}$$

and either condition (8.19) or condition (8.20):

$$0 \leq -\frac{\text{sign}\,(\Delta_{j,i^*})}{\Theta_j} \quad \forall\, j \in L \tag{8.19}$$

$$0 > \min_{j \in L} \left\{ -\frac{\text{sign}\,(\Delta_{j,i^*})}{\Theta_j} \right\}. \tag{8.20}$$

When condition (8.19) is satisfied, the terminal regulator index $i^* \in L$. Otherwise, condition (8.20) is satisfied and $i^* \in H$.

A simple algorithm to identify the ending regulator i^* in the max–min case follows:

1. Assume that $i^* \in L$ and take $i^* = 1$.
2. Check condition (8.18). If true, check condition (8.19). If true, i^* is the ending regulator. If not, take the next $i^* \in L$ and re-check.
3. If the final regulator is not found in L, repeat the above steps, checking condition (8.20) instead of (8.19).

8.3 Summary of Stability Properties

In [59], a proof of global asymptotic convergence to the equilibrium point $\bar{x}_{\text{ai}}$ is developed that relies only on the assumptions stated at the outset. The proof is based on attractiveness properties of each individual sliding set, together with considerations about the geometry of the regions of $\mathbb{R}^{n+1}$ in which each regulator is active under any of the min, max or max-min switching logic. Here, the relevant stability properties are summarized, omitting the lengthier proofs. The reader is referred to [59] for detailed proofs.

8.3.1 Stability: Min or Max Switching

All trajectories of System (8.2), (8.3) under control input (8.7) and the min switching law converge asymptotically to the unique equilibrium point x_{ai^*}.
The property $\max\{u_{ri}\} = -\min\{-u_{ri}\}$ can be used to infer stability for the max case using the proof of the min case.

8.3.2 Stability : Max–Min Switching

The max–min case requires additional analysis, as index selection cannot be expressed in terms of min only. However, the property $\max\{a_k - b_j\} = \max\{a_k\} - \min\{b_j\}$ for any two collections of numbers $\{a_k\}$ and $\{b_j\}$ proves useful in reducing the proof to the already-studied min and max cases. An important property of the max–min arrangement is that there exists a finite time after which switching is restricted to happen either among the min or the max selectors, whichever group contains the terminal index. In what follows, and without loss of generality, it is assumed that the terminal regulator index belongs to the min set, that is, $i^* \in L$.

All trajectories of System (8.2), (8.3) under control input (8.7) and the max–min switching law converge asymptotically to the unique equilibrium point x_{ai^*}. Moreover, the total number of switchings from the L set to the H set is at most equal to the number of regulators in the H set.

8.4 Invariance Properties: Limit Protection

The results of this section show that the min, max, and max–min designs actually maintain outputs within limits. In summary, it will be shown that *when the min switching law is used alone, outputs whose* Θ *is positive will be protected against upper-limit violations and outputs whose* Θ *is negative will be protected against lower-limit violations. Conversely, the max switching law alone protects outputs whose* Θ *is positive against lower-limit violations and outputs whose* Θ *is negative against upper-limit violations.* A max–min scheme is used to cover additional combinations of signs of Θ and upper or lower limits.

Recalling the definitions of Sect. 7.2.1, an interval $(-\infty, b]$ is invariant for a generic real variable $z(t)$ if $\dot{z}(t) \leq 0$ at $z = b$. Similarly, an interval $[a, \infty)$ is invariant if $\dot{z}(t) \geq 0$ at $z = a$. When an interval is invariant and $z(t_1)$ belongs to the interval for some $t_1 > 0$, then $z(t)$ will remain in the interval for $t \geq t_1$. For the proposed technique to be effective, the interval $(-\infty, 0]$ must be invariant for the s_j of upper-limited variables, in view of the definition of s_j for limited output y_j. Conversely, $[0, \infty)$ must be invariant for the s_j of lower-limited variables.

8.4.1 Invariance Under Min Switching

Let y_j be a limited variable. The derivative of s_j when i is active is given by (8.15). When i is active, we must have $u_i \leq u_j$, so:

$$\frac{\dot{s}_{j|i}}{\Theta_j} = \Gamma_{j,i}\tilde{x}_a - \frac{\eta_i}{\Theta_i}\,\text{sign}\,(s_i) \leq -\frac{\eta_j}{\Theta_j}\,\text{sign}\,(s_j).$$

Noting that the inequality changes to equality for $j = i$, it is clear that $\frac{\dot{s}_j}{\Theta_j} \leq 0$ at $s_j = 0$ under *any* regulator. If $\Theta_j > 0$, upper-limit protection is guaranteed. If $\Theta_j < 0$, lower-limit protection is guaranteed.

8.4.2 Invariance Under Max Switching

Following the same reasoning used for the min case, it is clear that $\frac{\dot{s}_j}{\Theta_j} \geq 0$ at $s_j = 0$ under any regulator. If $\Theta_j > 0$, lower-limit protection is guaranteed. If $\Theta_j < 0$, upper-limit protection is guaranteed.

8.4.3 Invariance Under Max–Min Switching

One would expect that the max–min arrangement guarantee invariance of any real interval $[a, b]$ containing zero, regardless of the sign of Θ, but this is not the case. An exception occurs for s_j when $j \in L$ and the active regulator belongs to H. This lack of symmetry arises from the fact that for $q \in H$ to be active it is necessary that u_{rq} be greater than the *minimum* of all u_{rl}, $l \in L$, but not for every u_{rl} in L. In contrast, for $q \in L$ to be active, u_{rl} must be greater than *every* u_{rh}, $h \in H$. Indeed, suppose $q = i \in L$ is active and consider a variable s_j and its derivative along the boundary $s_j = 0$:

$$\dot{s}_{j|i}/\Theta_j = u_{\text{ri}} - u_{\text{rj}} - \eta_j\,\text{sign}\,(s_j)/\Theta_j = u_{\text{ri}} - u_{\text{rj}}. \tag{8.21}$$

If $j \in L$, it is necessary that $u_{\text{ri}} - u_{\text{rj}} \leq 0$, while one must have $u_{\text{ri}} - u_{\text{rj}} \geq 0$ if $j \in H$. Thus, while $q \in L$, s_j is upper-bounded by zero if $\Theta_j > 0$, and it is lower-bounded by zero if $\Theta_j < 0$. Now consider $q = i \in H$ to active. Equation (8.21) still applies. If $j \in H$, it is necessary that $u_{\text{ri}} - u_{\text{rj}} \geq 0$. Thus, while $q \in H$, all variables s_j *associated to the max selector* will be upper-bounded by zero when $\Theta_j < 0$ and will be lower-bounded by zero if $\Theta_j > 0$. The difficulty arises when considering $j \in L$ while the active regulator is in H. The difference $u_{\text{ri}} - u_{\text{rj}}$ may be positive,

negative or zero, and invariance does not apply. Fortunately, separate arguments can be made which maintain the validity of the approach under commonly found circumstances. These arguments are elaborated in the next section.

8.5 Additional Considerations

For the remainder of the article, it is assumed that regulators are assigned to selectors so as to exploit the invariance properties described above. These assignment rules have been summarized in Table 8.1.

8.5.1 Limited Output Consistency

The results of this chapter are directly applicable to setpoint changes, implying that initial and final plant states $[x^T|u]^T$ are equilibrium points. Then it is always possible to redefine variables so that the initial input u, state x, and outputs y_j are zero. Frequently, it occurs that the sign of the DC gain of the transfer functions from u to y for the limited outputs coincides with the sign of Θ. The steady plant input–output relationships have the form

$$\bar{y}_j = \Theta_j(1 - G_j A^{-1} B/\Theta_j)\bar{u}$$

for $j = 1...h$. If $1 - G_j A^{-1} B/\Theta_j > 0$, then the sign of steady input $\bar{u}$ will match that of the limit $\bar{y}_j$ when $\Theta_j > 0$ and will be of the opposite sign when $\Theta_j < 0$. This has useful implications for the behavior of min-variables when $q \in H$, where invariance was not found. The following heuristic reasoning applies: if $q \in H$ because an upper-limited variable from the max group is reaching its (positive) limit, then u will be negative, since Θ_j must be negative according to the assignment rules. Any y_i among the min-selected variables which is upper-limited will be driven away from its limit by the negative $\bar{u}$, since $\Theta_i > 0$ by the assignment rules. The same reasoning can be followed for other combinations. This behavior is confirmed in simulation.

Table 8.1 Guidelines for the association of sliding mode regulators to selectors

Limit	Sign of Θ	Selector
Upper	+	Min
Upper	−	Max
Lower	+	Max
Lower	−	Min
Regulated output	n.a.	min

8.6 Design Process

This paper deals with a single control input and a single controlled output, whose setpoint is to be changed. Of all outputs, exactly one is the controlled variable, while the rest are limited variables. The G_i and Θ_i for the limited outputs are given by the system definition and are thus not design freedoms. The fundamental assumption that they define minimum-phase outputs must hold for this technique to work, however. The designer may freely choose all switching gains η_i and the reference states $\bar{x}_i$ and $\bar{u}_i$ so that they constitute equilibrium pairs and so that they correspond to the desired setpoint for the controlled variable and to the limits $\bar{y}_i$. Next, upper-limited variables such that $\Theta_i > 0$ and lower-limited variables having $\Theta_i < 0$ are placed under the min selector, while upper-limited variables with $\Theta_i < 0$ and lower-limited variables such that $\Theta_i > 0$ are placed under the max selector, as summarized in Table 8.1.

For the purposes of showing stability, no distinction was made between regulated and limited outputs, and the sliding function for the regulated variable was defined as the difference between the output and a limit. Suppose $y_0 = C_0 x + D_0 u$ is the true system output to be regulated (i.e., fan speed). Since output setpoint regulation is equivalent to the selection of a reference pair $(\bar{x}, \bar{u})$, one may introduce a "limited" variable and associated regulator for the purpose of reaching the reference state. Without loss of generality, suppose that $y_1 = G_1 x + \Theta_1 u$ is such variable. For y_0 to reach its setpoint, $(\bar{x}_1, \bar{u}_1)$ must be chosen under the restriction that $G_1 \bar{x} + \Theta_1 \bar{u}$ equals the desired setpoint, and G_1 and Θ_1 must be chosen to satisfy the minimum-phase assumption and for good performance during the sliding mode. The regulator for y_1 is then placed under the min selector. Under nominal conditions, the designer ensures that $i^* = 1$, so that y_1 attains the commanded setpoint. This is easily accomplished by manipulation of Θ_1 and η_1, since the choices do not affect the ability to place the eigenvalues of $A_{\text{eq},1}$, nor compromise system stability.

8.6.1 MultiObjective Control: Mixed $\mathcal{H}_2/\mathcal{H}_\infty$ Feedback Gain Synthesis

Although the above alone will guarantee stability and limit protection in both transient and steady states, eigenvalue placement for $A_{\text{eq},1}$ using G_1 may be carried out under additional, performance-oriented constraints. The interaction among the controlled and limited variables may be minimized in the sense of a mixed-sensitivity $\mathcal{H}_\infty$ approach. Consider the following generic control system in state-space form:

$$\dot{x} = Ax + B_1 w + B_2 u \tag{8.22}$$

$$z_{i,\infty} = C_i x + D_{i,1} w + D_{i,2} u \tag{8.23}$$

$$z_{j,2} = C_j x + D_j u, \tag{8.24}$$

where $i = 1, 2, ..I$ and $j = 1, 2..J$ are the indices of performance outputs $z_{i,\infty}$ and $z_{j,2}$. The objective is to find a feedback gain K that:

1. Stabilizes (A, B_2) under the control input $u = -Kx$ and
2. Minimizes a weighted objective function of the form $\alpha||T_\infty||_\infty^2 + \beta||T_2||_2^2$,

where T_∞ is the closed-loop transfer matrix from the exogenous inputs w (i.e., disturbances) to the performance outputs $z_{i,\infty}$ and T_2 is the closed-loop transfer matrix from w to the performance outputs $z_{i,2}$. The weighting coefficients α and β reflect design priorities and may be set to zero. The subindices represent the infinity and 2-norms, respectively, which are commonly-used in the standard $\mathcal{H}_\infty$ and LQG problems [28, 29]:

$$||T_\infty||_\infty = \max_w \bar{\sigma}\left(T_\infty(jw)\right) \tag{8.25}$$

$$||T_2||_2^2 = \frac{1}{2\pi}\int_{-\infty}^{\infty} \text{trace}\left(T_2(jw)T_2^*(jw)\right)\text{d}w, \tag{8.26}$$

where $\bar{\sigma}$ denotes maximum singular value and * denotes complex-conjugate transpose. These norms were used in Chap. 4 as part of a robust state feedback gain synthesis approach.

Note that the performance outputs are stacked together, allowing the designer to include multiple objectives in the norm minimization. This generic problem may be solved with additional constraints, for instance the requirement that the eigenvalues of $(A - B_2K)$ lie in certain region of the complex plane. Software tools such as the `msfsyn` function within Matlab's Robust Control Toolbox are available to solve these problems.

In the context of aircraft engine controls, w may represent actual disturbances or may be used to capture the effects of engine aging and deterioration. In fact, matrix Γ in (8.2), representing the influence of health parameter perturbations, may be directly obtained by linearization. In the context of sliding mode control, w represents an *unmatched disturbance* if Γ does not belong to the column space of B [53, 55, 70]. This means that w cannot be regarded as an additive component to the control input u. Consequently, w may not be exactly canceled out by u even if it were known or accurately estimated. Since it cannot be assumed that health parameter perturbations will be of the matched type, a reasonable design objective is to minimize the influence of w on the regulated variable.

The generic multiobjective synthesis approach described above may be directly applied to guide the selection of G_1, the sliding coefficients for the main regulator. To do this, system dynamics under an ideal sliding regime with i^* as the active regulator are considered. Under these conditions, the control input has the state-feedback form $u = -Kx$, with $K = \frac{1}{\Theta_{i^*}}G_{i^*}$. The $\mathcal{H}_2$ objective is included by considering $z_{j,2} = y_{j|i^*}$. That is, the (transient) excursions of y_j under control input $u = -\frac{1}{\Theta_{i^*}}G_{i^*}x$ are to be minimized in an $\mathcal{H}_2$-sense. For this, the transfer functions of interest are of the form

$$T_{j,2}(s) = G_j(sI - A)^{-1}B + \Theta_j. \tag{8.27}$$

Note that T_2 is formed by stacking the $T_{j,2}$ together. Also note that T_2 in the generic problem regards w as the input. Here, $B_1 = B_2 = B$ has been used to reflect the intuitive requirement that u must not unduly excite y_j.

The $\mathcal{H}_\infty$ objective is included by considering a single performance output $z_{i^*,\infty} = y_{i^*}$. The corresponding transfer function is

$$T_{i^*,2}(s) = C_0(sI - A)^{-1}B_1 + D_0, \tag{8.28}$$

where C_0 and D_0 define the regulated output. Note that $G_{i^*} \neq C_0$ and $\Theta_i^* \neq D_0$ in general.

8.7 Design Examples

8.7.1 Linearized Simulation Study

We consider the problem of changing fan speed between two setpoints with limits in T_{48}, EPR, high-pressure compressor stall margin (SmHPC), and HPC exit static pressure (Ps30). Note that no real-time sensing of the stall margin is possible, however the SM controller only requires fan and core speeds as feedback measurements. The CMAPSS model linearized at flight condition FC07 listed in Appendix B is used.

This system is open-loop stable, so the assumption that A is nonsingular is satisfied. We consider the excursions of EPR and T_{48} from the values in Table 2.3 to be upper limited at 0.35 and 400°R, respectively, while those of Ps30 and SmHPC to be lower-limited at −85 psia and −15%. The values of the limits are representative of actual engine operations. These limited outputs are defined as in (8.4) with

$$\begin{aligned} G_2 &= [0.0071 \;\; 0.0177], & \Theta_2 &= -18.4743 \\ G_3 &= [0.0244 \;\; -0.2665], & \Theta_3 &= 410.4741 \\ G_4 &= [-0.0037 \;\; 0.1599] \times 10^{-3}, & \Theta_4 &= 0.0461 \\ G_5 &= [0.0017 \;\; 0.0855], & \Theta_5 &= 25.5719, \end{aligned}$$

where indices 2, 3, 4, and 5 correspond to SmHPC, T_{48}, EPR, and Ps30, respectively. It can be verified that these outputs are minimum-phase, satisfying the minimum-phase assumption. Given a fan speed increment setpoint and the set of limits, the corresponding reference states $(\bar{x}_i, \bar{u}_i)$ are readily computed by enforcing equilibrium conditions and using the output definitions, that is

$$\begin{aligned} A\bar{x}_i + B\bar{u}_i &= 0 \\ G_i\bar{x}_i + \Theta_i\bar{u}_i &= L_i, \end{aligned}$$

where L_i are the values of the limits. Note that the reference states for the fan speed regulator are found using $C_1 = [1 \; 0]$, $D_1 = 0$, and L_1 equal to the desired setpoint

for ΔN_f. However, the fan speed regulator does not use C_1 and D_1 as sliding function coefficients, since limit preservation is not required for this variable. To find G_1 and Θ_1, we solve the $\mathcal{H}_2$ minimization with regional eigenvalue placement described in the design section. The optimization is carried out with the `msfsyn`, which is part of Matlab's Robust Control Toolbox. The eigenvalue placement region was specified as the half-space $\mathrm{Re}(s) \leq -4$. Setting $G_1 = 1$ arbitrarily, the solution returns

$$G_1 = [0.0118 \;\; 0.0026],$$

which places the eigenvalues of $A_{\mathrm{eq},1}$ at -5.26 and -4.40. The regulators are now associated with the min or max selectors according to Table 8.1. The fan speed regulator is applied to the min regulator. Since $\Theta_2 < 0$ and y_2 is lower-limited, the output limit regulator #2 is applied to the min selector. Similarly, since Θ_3 and Θ_4 are positive and y_3 and y_4 are upper-limited, the corresponding regulators are applied to the min selector. Finally, $\Theta_5 > 0$ and y_5 is lower-limited, so the regulator is associated with the max selector. Under nominal conditions, the designer wishes that #1 be the terminal regulator. Since the only controller parameters left to be specified are the switching gains $\eta_i > 0$, and because their choice does not compromise stability, tuning is straightforward and requires little or no iteration. The η gains are adjusted until $i^* = 1$ is predicted and a satisfactory response is observed in simulation. For this example, it can be verified that setting $\eta_i |\Theta_i| = 15$ for $i = 1, 2, 3, 4, 5$ results in $i^* = 1$.

Figures 8.2 and 8.3 show fan speed and auxiliary output responses to a setpoint of $\Delta N_f = 340$ rpm with all limit regulators disabled. As expected, it can be observed that y_1 attains its setpoint; however, some auxiliary variables exceed their limits. Specifically, T_{48} and SmHPC incur transient violations. EPR does not reach its limit, and Ps30 has a DC gain of the opposite sign as N_f, causing it to move away from its lower-limit. Note that the settling time for N_f is about 1 s.

Figures 8.4 and 8.5 show the responses obtained when the limit regulators are enabled. It can be seen that T_{48} and SmHPC now "ride" their limits during the transient regime. Naturally, the fan speed response will show some performance degradation in terms of transient behavior, but its ability to reach the setpoint will not be hindered, since the design ensures that $i^* = 1$ under nominal conditions. The settling time is now about 1.4 s. Note that the limit $\Delta T_{48} = 400°\mathrm{R}$ has been made very "tight" for illustrative purposes. Considering that the absolute limit on T_{48} used in realistic engine controls is close to 2,200°R, Table 2.3 indicates that ΔT_{48} could be chosen as high as 657°R. Under these conditions, the same design would result in a faster settling time.

To illustrate activation of the lower limit, suppose now that fan speed is to be reduced, that is, the setpoint is $\Delta N_f = -340$ rpm. It can be verified that $i^* = 1$ and $i_0 = 1$ still hold under the same design parameters. Figures 8.6 and 8.7 show that Ps30 reaches its lower limit and holds it for some time.

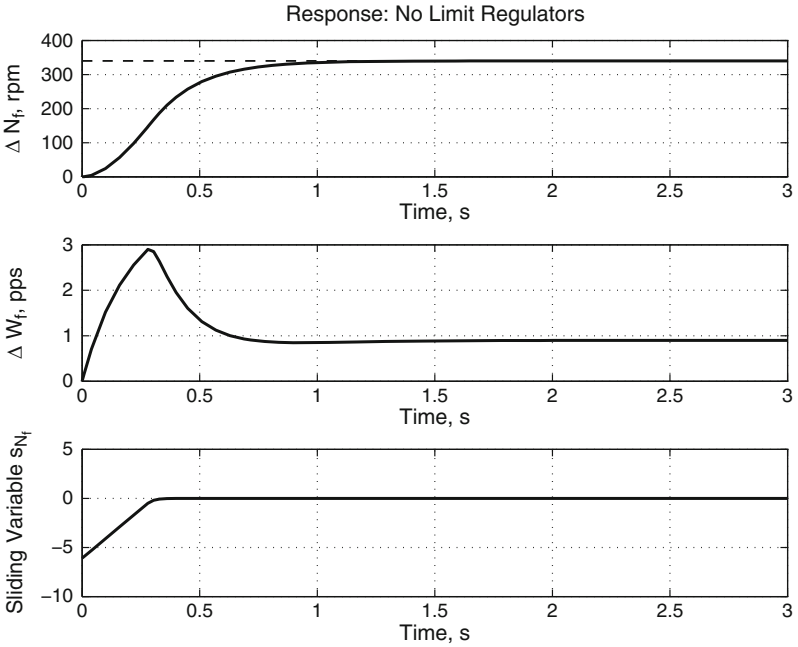

Fig. 8.2 Fan speed response with limit regulators removed: positive setpoint change

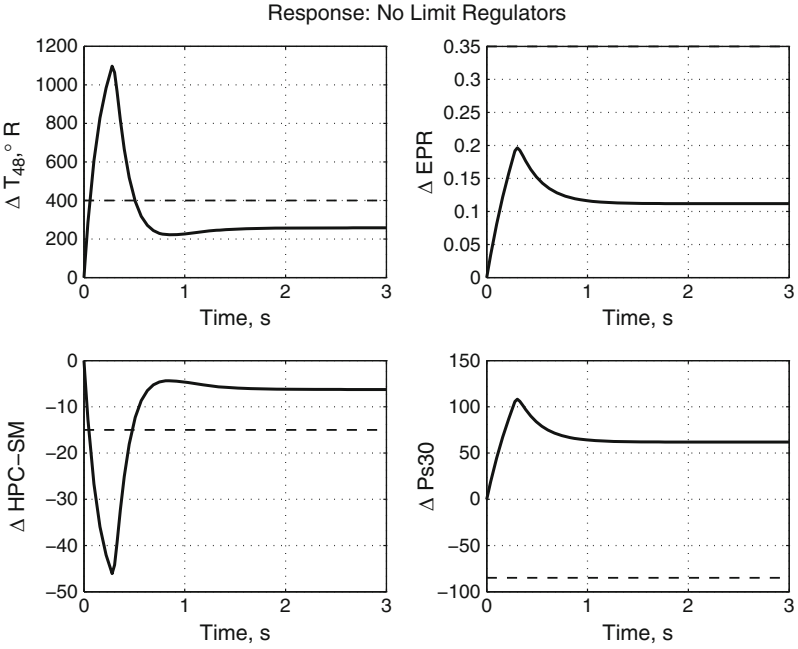

Fig. 8.3 Auxiliary output response with limit regulators removed: positive setpoint change

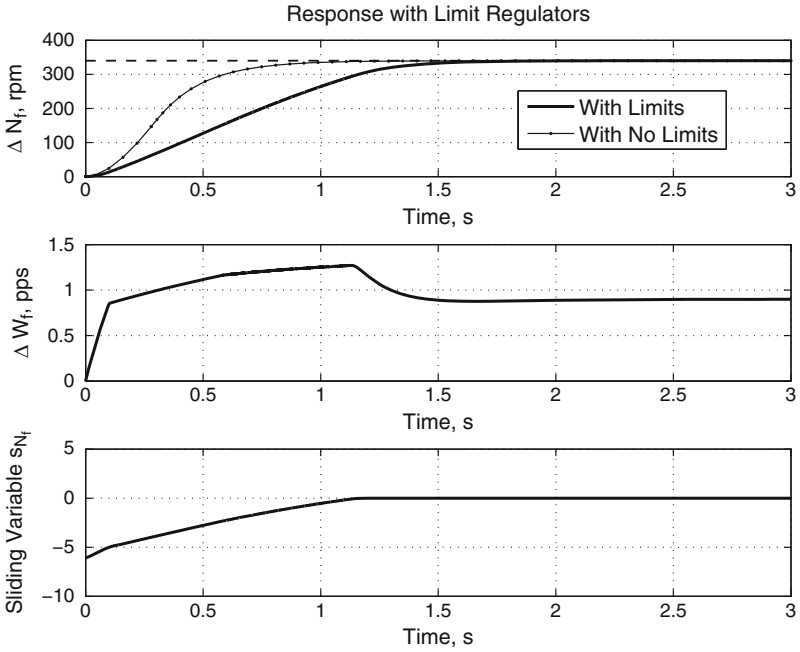

Fig. 8.4 Fan speed response with limit regulators enabled: positive setpoint change

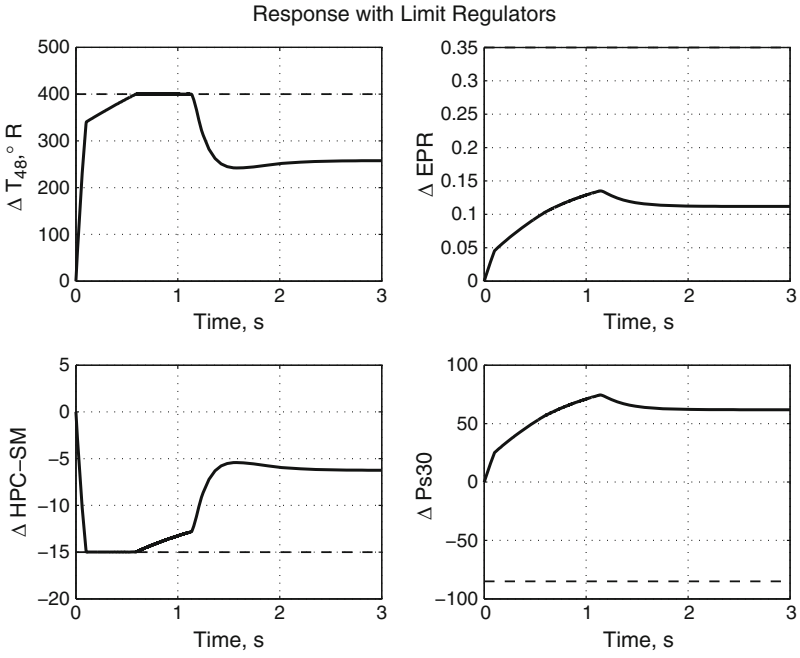

Fig. 8.5 Auxiliary output response with limit regulators enabled: positive setpoint change

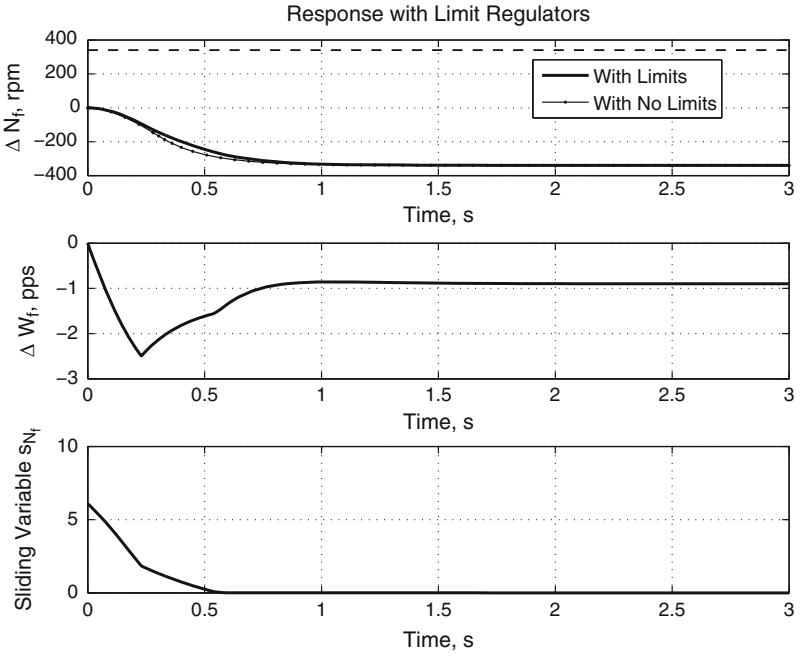

Fig. 8.6 Fan speed response with limit regulators enabled: negative setpoint change

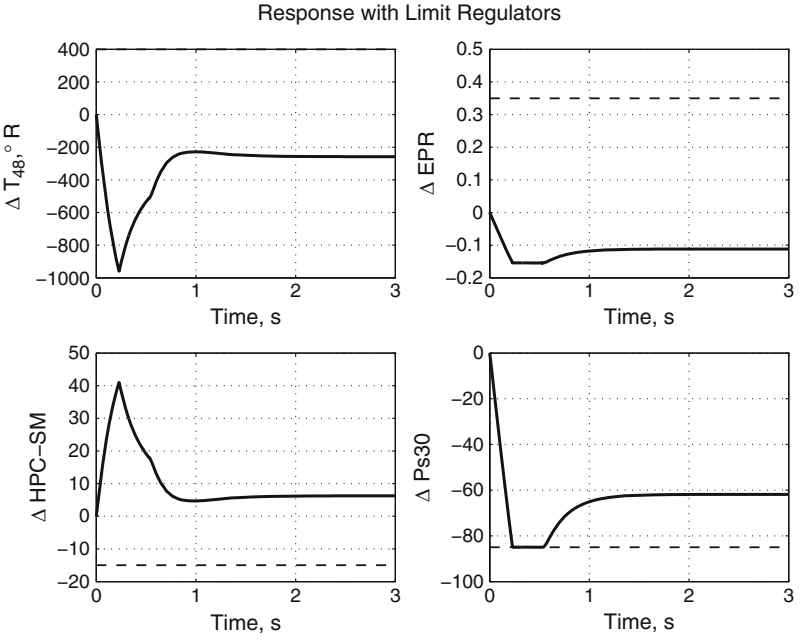

Fig. 8.7 Auxiliary output response with limit regulators enabled: negative setpoint change

8.7.2 CMAPSS Implementation: Upper Limit on T_{48}

The above example was meant to illustrate the details of the design process. The simulations used linearized models, however. The simulation studies of this section are conducted in CMAPSS-40k, and strongly suggest that the combination of sliding mode regulators and max–min selectors is robust enough to produce satisfactory responses and limit protection behavior when applied to a high-fidelity nonlinear engine simulation. In turn, the nonlinear simulation provides evidence for the feasibility of this technique to be deployed in real-time to an actual engine. Note that the control law of (8.7) carries an insignificant computational burden, especially when compared to other control strategies aiming to handle constraints, like model predictive control. In this example, minimizing the effects of health parameter changes is also included among the design objectives. A fan speed regulator and a T_{48} regulator are considered, both associated with a single min selector. The increment request for N_f is the same as in the previous example, but the T_{48} limit is reduced to 1,900°R ($\Delta T_{48} = 357$°R to study the behavior of each design under tight limits. Among the health parameter perturbations discussed in Sect. 8.1, the HPT flow modifier and the HPT efficiency modifier have the largest influence on T_{48}. They correspond to a specific Γ matrix (see (8.2)), obtained during linearization. At the flight condition considered in this example matrix Γ is given by:

$$\Gamma = \begin{bmatrix} -505.4 & 152.6 \\ 4325.2 & -1030.5 \end{bmatrix}.$$

Step changes from 0% to 3% in each component of w will be considered in the CMAPSS example, simulating the effect of a sudden fault. A comparison is to be made between the proposed design and the max–min strategy with linear regulators, which is the default in CMAPSS. Each linear regulator (including that for the regulated output) is designed using the so-called KQ technique due to Edmunds [27]. In summary, each regulator is restricted to be of the lead-lag type. The pole of the regulator is arbitrarily set, and the zero and the gain are found by model-matching optimization, whereby the closed-loop system is required to meet a target closed-loop bandwidth w_b and damping ratio ζ for a pair of dominant poles. Although this classical technique may be satisfactory for independent loops, it does not incorporate any information about the interaction of the regulators through the max–min selector, nor does it use information about the values of the setpoints or limits. As a result, poor performance may be observed, even when a limited variable stays far from its limit. For illustrative purposes, a KQ design was conducted using $\zeta = 0.7$ and $w_b = 4$ rad/s, which according to classical compensation design techniques [26] should produce a settling time of 1.45 s assuming that the regulator is active at all times. These parameters and a real pole at $s = -20$ were used for both N_f and T_{48} regulators. The resulting compensators are

$$K_{N_f}(s) = \frac{0.1196s + 0.1868}{s + 20}$$

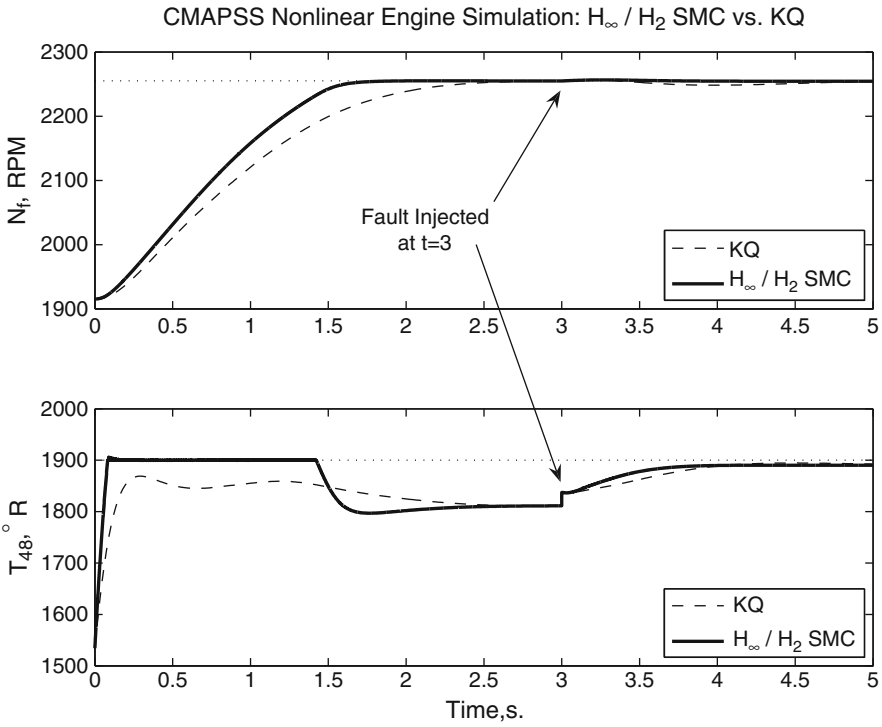

Fig. 8.8 CMAPSS simulations: Fan speed response with T_{48} limit regulator and simulated fault

$$K_{T_{48}}(s) = \frac{-0.01017s + 0.1073}{s + 20}.$$

Note that the KQ design introduces a right-half plane zero in the T_{48} loop, raising concerns about the general validity of Edmunds' approach. Separately, a sliding mode max–min design with mixed $\mathcal{H}_2$ norm minimization was carried out, following the same steps as in the previous example, including performance output z_∞ to capture the effects of w on N_f. The regional pole placement constraint was maintained, this time using $\mathrm{Re}(s) \leq -5$. Finally, $\alpha = 1$ and $\beta = 1$ were used. The resulting sliding coefficient vector for the N_1 regulator was $G_1 = [0.0168 \;\; 0.0014]$, with Θ_1 arbitrarily set to 1. The eigenvalues of $A_{\mathrm{eq},1}$ are $-5.0112 \pm 1.5396i$. The switching gains were set at $\eta_1|\Theta_1| = \eta_2|\Theta_2| = 15$. The resulting controller was implemented in CMAPSS, and a sample comparison simulation was run. The results are summarized in Figs. 8.8 and 8.9. It is clear that the new design outperforms KQ by a large amount in terms of fan speed response, maximization of the available limit, and low sensitivity to a simulated fault. Note that the settling time with the proposed design is 40% shorter than the one obtained with the KQ design. The example also indicates that a design based on a linearized plant is adequate for deployment to the nonlinear model, although scheduling or gain adaptation is likely

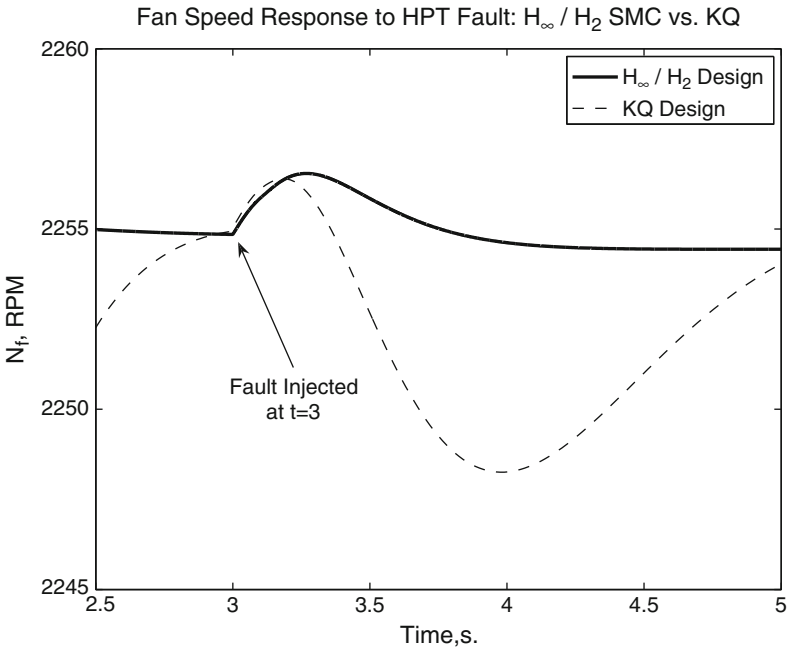

Fig. 8.9 Detail of Fig. 8.8: Response to fault input

to be necessary to cover the whole flight envelope or to accommodate larger setpoint changes.

8.7.3 CMAPSS Implementation with Multiple Limit Regulators

In this example, a more realistic implementation of the max/min SMC approach is described. As in the simulation example, T_{48} and EPR are regarded as upper-limited and Ps30 as lower-limited. A limit regulator cannot be directly implemented for the stall margin, however, since this output is not sensed in the actual engine. A related variable usually referred to as Φ can be used instead to achieve a minimum stall margin requirement. This variable is defined as the ratio of fuel flow rate to static HPC outlet pressure Ps30:

$$\Phi = \frac{W_F}{\text{Ps30}}.$$

An allowable range for the value of Φ is typically used to calculate corresponding allowable values of W_F on the basis of the current value of Ps30 [71]. That is, the value of W_F calculated by the control system is passed through a saturation function with variable limits which are determined from the minimum and maximum values allowed for Φ and the current value of Ps30. In this example, however, we consider

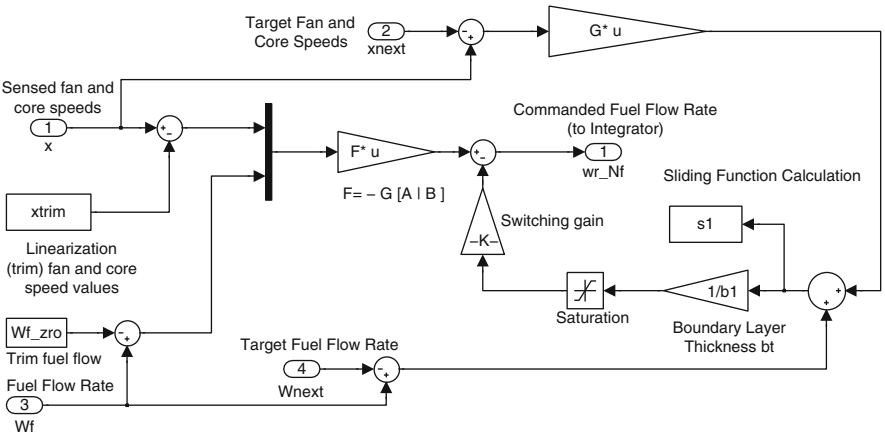

Fig. 8.10 CMAPSS simulation diagram for max–min/SMC: Main output regulator

only an absolute lower limit on Φ, enforced by an SMC limit regulator. Since the D coefficient of the linearized output $\Delta\Phi$ is positive, the limit regulator is associated to the max selector. Note that if an upper limit is specified for Φ in addition to the lower limit, an extra regulator must be associated to the min selector.

The example corresponds with a burst and chop maneuver starting at FC07. A fan speed demand is created that corresponds to a step increase in TRA from 60 to 100°. The opposite TRA change is used for the chop portion. The sliding coefficients for the main output regulator are determined using the $\mathcal{H}_2/\mathcal{H}_\infty$ approach. Fan speed is regarded as the z_∞ performance output and z_2 includes all limited outputs. Equal weights for the $\mathcal{H}_2$ and $\mathcal{H}_\infty$ objectives are specified, and the target eigenvalue region is taken as a disk centered at -8 with radius 2.

The sliding coefficients returned by `msfsyn` are

$$G = [0.0452 \quad -0.0010],$$

which places the poles of A_{eq} at -9.99 and -6.00. The design is completed by specifying a set of switching gains that provide an adequately fast response while ensuring that the fan speed regulator is active at steady state. The switching gain for the main regulator was chosen as $\eta_1 = 1$, while $\eta_j = 15|\Theta_j|$ was chosen for all limit regulators. Boundary layer thickness parameters must be chosen according to orders of magnitude projected for the s variables. $\phi = 0.5$ was chosen for the main SMC regulator, together with $\phi_2 = 0.01$, $\phi_3 = \phi_4 = \phi_5 = 0.1$.

Figures 8.10 and 8.11 show the Simulink implementations of the main and limit regulators, where the T_{48} regulator has been used as an example of the latter. Figure 8.12 shows the behavior of the system state and main sliding function. The fan speed response has a fast settling time of about 0.8 s.

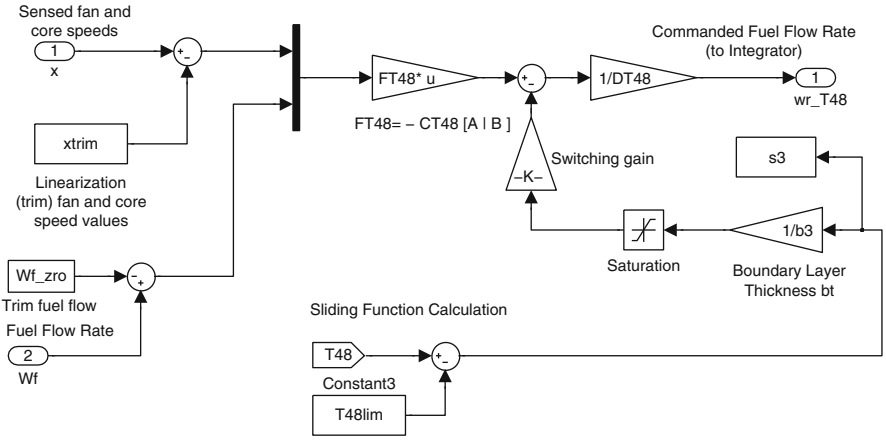

Fig. 8.11 CMAPSS simulation diagram for max–min/SMC: Limited output regulator

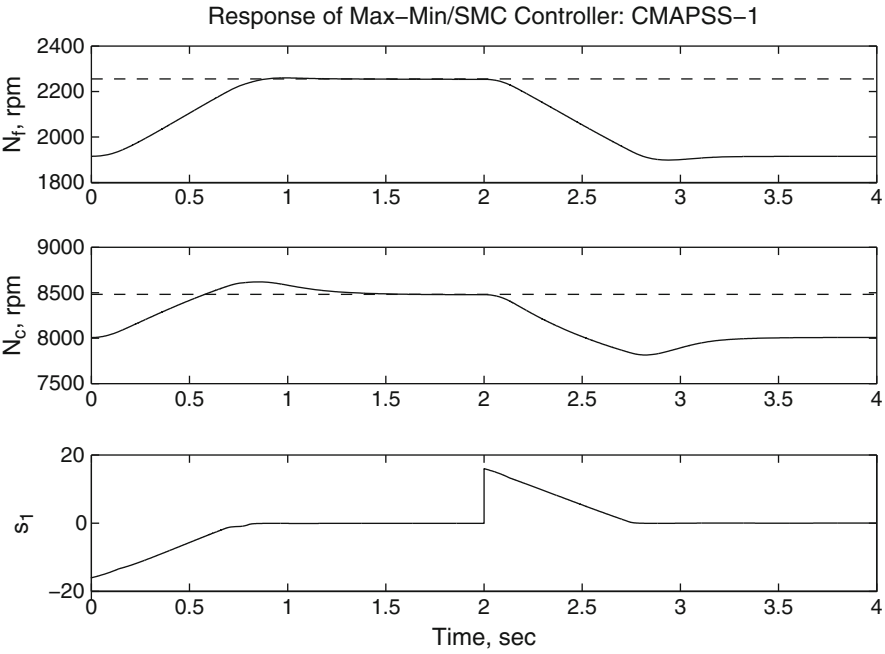

Fig. 8.12 CMAPSS simulation of max–min/SMC with $\mathcal{H}_2/\mathcal{H}_\infty$ tuning: State variable and sliding function responses

As shown in Fig. 8.13, T_{48} tends to peak during the burst transient, but SMC limit regulator effectively maintains the variable at the exact value of the limit (2,175°) as long as necessary. Similarly, Φ tends to undershoot pronouncedly during the chop

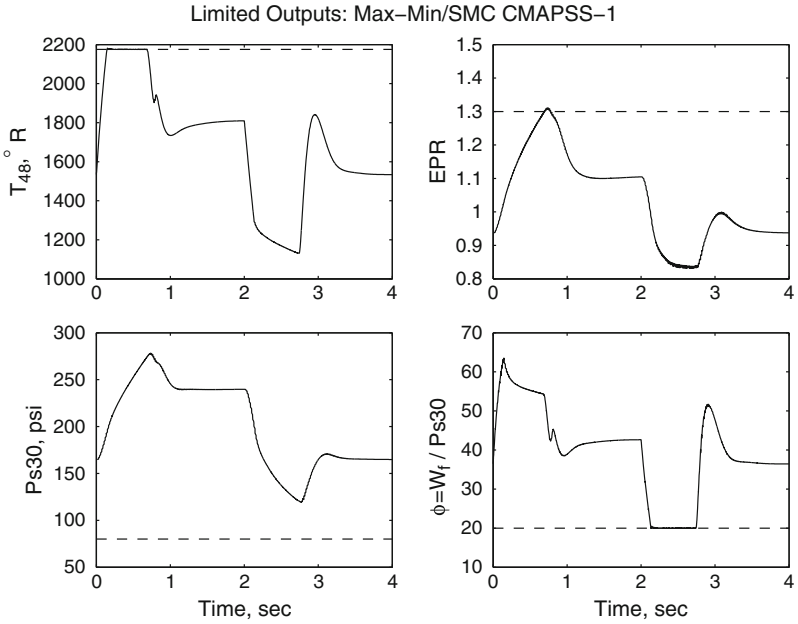

Fig. 8.13 CMAPSS simulation of max–min/SMC with $\mathcal{H}_2/\mathcal{H}_\infty$ tuning: Limited output responses

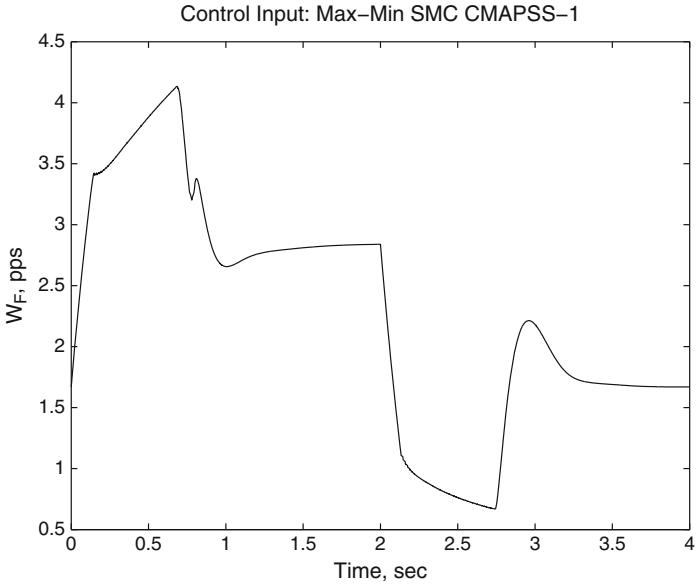

Fig. 8.14 CMAPSS simulation of max–min/SMC with $\mathcal{H}_2/\mathcal{H}_\infty$ tuning: Fuel flow input

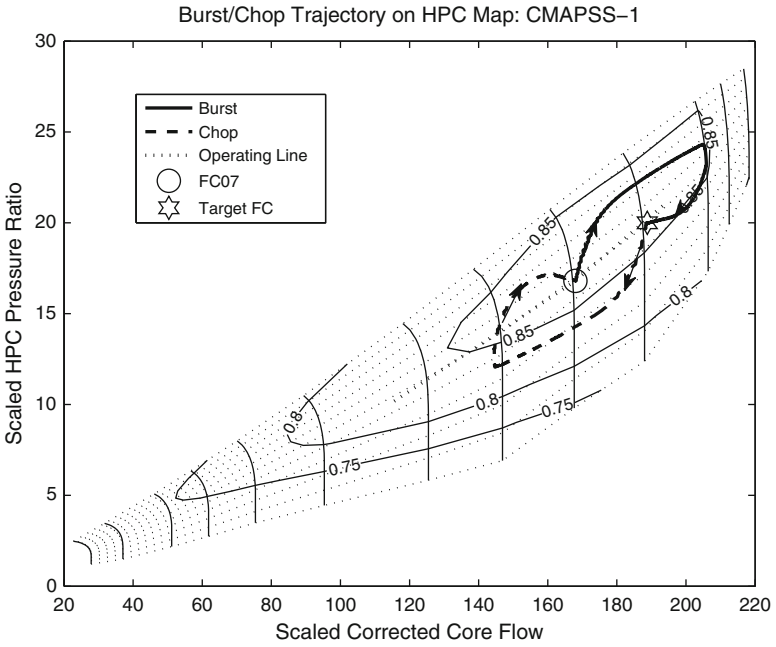

Fig. 8.15 CMAPSS simulation of max–min/SMC with $\mathcal{H}_2/\mathcal{H}_\infty$ tuning: Representation of burst/chop trajectories on HPC map

transient, but is effectively held at the limit of 20 by its regulator. An upper limit of 1.3 was specified for EPR. Since the designer has no control over the sliding mode dynamics for the limit regulators, small oscillations around the limit value may be observed in a nonlinear engine simulation. This is the case with EPR: even if this regulator is forced to remain active at all times, convergence to $s = 0$ is not one-sided, but contains some oscillation. This explains the slight overshoot observed for EPR in Fig. 8.13. Figure 8.14 shows the fuel flow input produced by the control system. No significant chattering is detected, despite the high regulation accuracy of this system. Finally, the burst and chop sequence has been represented in the HPC map in Fig. 8.15.

8.8 Summary

The above CMAPSS implementations demonstrate the effectiveness of the max–min arrangement with SM regulators. The designer can use this technique to achieve a balance between speed of response and allowable limits for critical engine variables. Even with constant control gains, limit relaxation will be reflected in faster responses, and conversely, the main output response will become slower if

limits are made more restrictive. This feature is highly desirable for the development of *resilient aircraft control systems*, where the engines feature aggressive control modes reserved for emergency maneuvers. In emergencies, extending engine life becomes secondary to achieving enhanced thrust response. Indeed, recent aviation safety research [69,72] indicates that thrust response times determine the feasibility of certain emergency maneuvers where the propulsion system is used for flight control. In one scenario where all rudder control has been lost, the pilot commands different levels of thrust to the engines to achieve a yawing moment. Studies indicate that the control system must feature fast thrust response modes to be used in emergencies. In these situations, enhanced response must be favored over engine durability, while still guaranteeing component safety.

On the premise that the standard max–min architecture is used for both normal and enhanced responses, there are essentially two ways of obtaining faster thrust responses: (a): redesigning the regulators for larger closed-loop bandwidths; and (b): relaxing the protective limits on variables which tend to peak as thrust response is made faster. Among the variables displaying such peaking are turbine outlet temperature, which peaks during acceleration, stall margin, which tends to undershoot during acceleration, and combustor pressure, which tends to undershoot during deceleration. Unfortunately, the max-min arrangement with linear regulators introduces an undesirable relationship between design bandwidths, limit settings and the achieved speed of response. This observation was first made by Litt [69] and confirmed by the author in a simulation study [73]. The same study demonstrates that the max-min arrangement with SM regulators removes this limitation.

The technique presented in this chapter requires the specification of augmented state references, which includes target steady values for the actuators, since integral control is used. As mentioned in Sects. 4.7.1 and 6.3, the steady map of the nonlinear engine must be used to pre-calculate such references. This drawback is aggravated when health parameter changes occur, since the steady map depends on these uncertain parameters. Note, however, that real-time implementations of the SM limit regulators do not require state references, due to the definition of the sliding function. Only the limit setting and a real-time output measurement are needed to calculate the sliding function.